EXPERIMENTAL STUDY ON RADIAL DECOUPLING CHARGE BLASTING WITH AIR AND WATER

Deqiang YANG[1], Huaming AN[2]*,
Zhen LEI[3]

[1] Civil and Resource Engineering School, University of Science and Technology Beijing, Beijing, 100083, China
[2] Kunming University of Science and Technology, Kunming, 650093, China
[3] Guizhou Institute of Technology, Guiyang, 550003, China

Abstract: In order to investigate the effects of the different medium on the initial impact pressure and fragmentation of the hole wall under radial decoupling charge, this paper analyzes and compares the initial impact pressure of hole wall and the size of blasting lumpiness theoretically when air and water are used as a coupling medium. Combined with blasting model test, strain datas are collected by high-speed multi-channel dynamic stress testing system, and the lumpiness of the model test is sieved and measured. The blasting lumpiness is analyzed by *G–G–S* distribution function. The results show that compared with the air radial decoupling charge, the water radial decoupling charge has higher blasting peak pressure and more uniform lumpiness. According to the relation between peak strain pressure and decoupling coefficient, the optimal decoupling coefficients of air and water are 1.71 and 1.67, respectively. The results show that the best blasting effect can be achieved by using a small hole diameter of water-decoupling charge compared with air-decoupling charge. When the decoupling coefficient is 1.50, the average lumpiness size, distribution of large block and boulder yield of blasting lumpiness in water-decoupling medium are minimum, and only the average lumpiness size and distribution of large block are minimum in air-decoupling medium. Applying the test results to the smooth blasting of cutting has certain guiding significance for improving the blasting effect.

Keywords: *radial decoupling charge, concrete model, strain, blasting lumpiness, boulder yield*

1. INTRODUCTION

Decoupling charge technology has been widely used in blasting engineering practice. Compared with conventional charge technology, it can not only reduce blasting cost but also effectively improve blasting quality and effect. For cutting slope excavation, decoupling charge blasting excavation method is currently used, and blasting lumpiness is one of the most important indexes to evaluate blasting effect. Different blasting operations have different requirements on the size of blasting lumpiness, and earthwork blasting requires reducing the boulder yield and facilitating the transportation of earthwork.

Zong et al. (2003; 2004; 2012) carried out the theoretical analysis, laboratory test and field test on the impact pressure on pore wall and rock failure range of water-uncoupled medium. Dai et al. (2008) obtained the relation between the size of rock blasting lumpiness and the blasting pressure in the hole by theoretical derivation. Du et al. (2003; 2005) have theoretically analyzed the propagation of shock waves in a water-decoupled medium and the impact pressure of air-decoupled holes. Wan et al. (2003) made a theoretical analysis of the calculation of the initial impact pressures of five kinds of decoupled charges Ling W.M. (2004) used the manganese copper piezoresistive sensor and pulse constant current source test system to test the initial impact pressure of cement mortar and plexiglass medium under the condition of coupling and decoupling charge, and obtained the initial impact pressure value of hole wall at each point, which provides a reference for the direct measurement of this value. Yan et al. (2009) used LS-DYNA to establish a decoupling charge model for numerical simulation and analyzed the functional relationship between hole wall stress and decoupling coefficient under air-water-decoupling charge. Jiang et al. (2015) optimized the relationship between the unit consumption of blastings and the medium boulder yield and small boulder yield in the basic data of rock detonability classification. Liu et al. (2005) analyzed the distribution of blasting lumpiness under the coupling charge. Cai et al. (2014) studied the effect of decoupling coefficient of water-decoupling charge on the energy of stress wave in the near and far regions of deep-hole blasting. Yang et al. (1996) carried out air-decoupling charge blasting on cement mortar concrete to optimize decoupling coefficient. Sun et al. (2010) applied water-decoupling charge in coal mine laneway and achieved good results. Chen et al. (2015) discussed the selection basis of lumpiness evaluation index.

For the effect of decoupling charge on rock impact pressure and blasting lumpiness, based on the research results of predecessors, the initial impact pressure of hole wall and the size of blasting lumpiness in air and water are compared theoretically. Through the model test, change the decoupling coefficient, the initial impact pressure of hole wall and the blasting lumpiness are verified by regression analysis, and the test results are applied to cutting smooth blasting, which has certain guiding significance for improving blasting effect.

2. THEORETICAL BASIS

2.1. ANALYSIS OF THE INITIAL IMPACT PRESSURE ON THE HOLES
OF DECOUPLING CHARGES WITH DIFFERENT MEDIUMS

The relation between the gas static pressure p_0 and the decoupling coefficient K_d of the radial air-decoupling charge when the blasting gas expands and fills the whole hole is (Zong et al. 2003):

$$p_0 = n\frac{1}{8}\rho_e D^2 \left(\frac{d_c}{d_b}\right)^6 = n\frac{1}{8}\rho_e D^2 K_d^{-6}, \tag{1}$$

where: ρ_e is the density of the blasting, $g \cdot cm^{-3}$, D is the detonation velocity, $m \cdot s^{-1}$, d_c is the charge diameter of the borehole, cm, d_b is the hole diameter, cm, n is the multiple of the pressure increase when the detonation product collides with the hole wall, $n = 8\sim11$.

When detonation is initiated by the water-decoupling charge in the hole direction of the gun, the pressure at which the compression amount of water under the action of high blasting pressure reaches the limit is equal to the pressure of the detonation product. Set the compression amount of water is δ, according to the conservation of mass, the density of compressed water ρ_w' is (Zong et al. 2003):

$$\rho_w' = \frac{\left(r_b^2 - r_c^2\right)\rho_w}{r_b^2 - \left(r_c + \delta\right)^2}, \tag{2}$$

where: ρ_w is the original density of water, $g \cdot cm^{-3}$, r_b and r_c are the hole radius and the hole charge radius, cm.

Bringing $K_d = \dfrac{r_b}{r_b}$ into formula (2) for further substitution to obtain:

$$\rho_w' = \frac{\left(K_d^2 - 1\right)\rho_w}{K_d^2 - \left(\dfrac{r_c + \delta}{r_c}\right)^2}. \tag{3}$$

Blasting gas is regarded as adiabatic expansion process, and its expansion pressure varies as follows:

$$p_x = n\frac{1}{8}\rho_e D^2 \left(\frac{r_c}{r_c + x}\right)^6, \tag{4}$$

where x is the radial compression of water, cm.

The pressure of the blasting gas at equilibrium (i.e., $x = \delta$) is:

$$p_b = n\frac{1}{8}\rho_e D^2 \left(\frac{r_c}{r_c + \delta}\right)^6 .$$ (5)

Combining formulas (3) and (5) yields formula (6):

$$p_b = n\frac{1}{8}\rho_e D^2 \left[\sqrt{K_d^2\left(1 - \frac{\rho_w}{\rho_w'}\right) + \frac{\rho_w}{\rho_w'}}\right]^{-6} .$$ (6)

Comparing formulas (1) and (6), formula (7) is obtained:

$$\frac{p_b}{p_0} = \left[\sqrt{\frac{K_d^2\left(1 - \frac{\rho_w}{\rho_w'}\right) + \frac{\rho_w}{\rho_w'}}{K_d^2}}\right]^{-6} .$$ (7)

According to the analysis of formula (7), the density of the water medium compressed by the blasting stress wave must be larger than the original density, so: $\rho_w/\rho_w' < 1$. As the decoupling charge $K_d > 1$, then

$$\frac{p_b}{p_0} = \left[\sqrt{\frac{K_d^2\left(1 - \frac{\rho_w}{\rho_w'}\right) + \frac{\rho_w}{\rho_w'}}{K_d^2}}\right]^{-6} > 1$$

is necessary, so: $p_b > p_0$.

According to the above analysis, the pressure of blasting gas in water medium is higher than that in air medium. The results show that the water-decoupling charge is easier to break the rock.

2.2. ANALYSIA OF THE EFFECT OF DECOUPLING CHARGES WITH DIFFERENT MEDIUMS ON THE BLASTING LUMPINESS

In reference (Dai et al. 2008), the relation between the size of rock blasting lumpiness d and the blasting load p_0 in the rock caused by charge blasting in the hole is pointed out:

$$d = \left[\sqrt{20}K_{IC}/(\rho c)\right]K^2\left(p_0(r/r_b)^{-\alpha}\right)^{-2} ,$$ (8)

where: K_{IC} is the fracture toughness of rock, MPa·m$^{1/2}$, ρ is the lumpiness density of the rock, N·m^{-3}, c is elastic wave velocity of rock, m·s^{-1}, K is a coefficient related to rock properties, r is the distance from the calculation point to the charge centre, cm, α is the attenuation index of blasting stress wave in rock, r_b is the radius of the hole, cm.

As can be seen from formula (8), $d \propto p_0^{-2}$. When the rock lumpiness size decreases by 2 levels, the size changes from d to $d/2$:

$$d/2 \propto p_0^{-2}/2 = \left(\sqrt{2}p_0\right)^{-2}. \tag{9}$$

Derived from formula (9):

$$\frac{d_b/2}{d_0/2} = \frac{\left(\sqrt{2}p_b\right)^{-2}}{\left(\sqrt{2}p_0\right)^{-2}}, \tag{10}$$

where: d_b is the lumpiness size underwater medium blasting, mm, d_0 is lumpiness size for air medium blasting, mm.

According to the above analysis, the size of blasting lumpiness in water medium is smaller than that in air medium under the same initiation condition, which indicates that the utilization rate of blasting energy by water-decoupling charge is higher and the blasting effect is better.

In conclusion, through the theoretical analysis and comparison of the initial impact pressure and blasting block size of the hole wall when air and water are used as the coupling medium, it can be concluded that the uncoupled charging of water is easier to break the rock and more conducive to improving the blasting effect.

3. MODEL TEST OF DECOUPLING CHARGE BLASTING IN DIFFERENT MEDIUMS

3.1. PRINCIPLE AND SYSTEM OF STRESS MEASUREMENT

The test is based on the principle of resistance strain. When the specimen is subjected to dynamic stress, the strain gauge pasted on the measuring point will produce corresponding strain along with the deformation of the specimen, which will cause the change of resistance. The strain of the specimen can be inversely calculated by converting the change of resistance into the change of voltage or current and recording the change of voltage or current with a display instrument. The calculation method is as follows (Han 2013):

$$\varepsilon = \frac{4U}{kU_0A}, \tag{11}$$

where ε is the strain of the specimen, U is the output voltage, V, k is the sensitivity coefficient of the instrument, $k = 2.00$, U_0 is instrument bridge pressure, V, $U_0 = 2V$, A is the instrumentation gain, set to 100.

Combined with Hooker's law: $P = \varepsilon E$, the stress at each point can be obtained, which P is the stress value, MPa.

As the data acquisition equipment, the strain gauge is pasted on the prefabricated strain brick and embedded in the concrete model as the sensor to receive the explosion signal. The instrument is shown in Fig. 1.
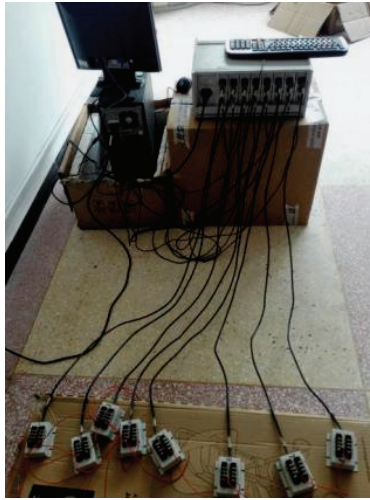

Fig. 1. Test system for stress monitoring

3.2. PREPARATION OF CONCRETE MODEL

According to the "Code for Construction and Acceptance of Concrete Structures" (GB50204-2015) and "Code for Design of Mixture Ratio of Concrete" (JGJ55-2011) and other relevant national standards and blasting similarity criteria, the strength of the model concrete is C30. The model material is poured by P.O42.5 ordinary Portland cement, sand, macadam and water according to the mass ratio of 1 : 1.556 : 3.158 : 0.52. The size of the concrete model is $30 \times 30 \times 30$ cm. There are five holes in the centre of the test block with the depth of 15 cm and the diameter of 1.0, 1.2, 1.4, 1.6 and 1.8 cm, respectively, which were cured for 28 days. There are ten concrete models. The model design and specimens are shown in Figs. 2 and 3.

Strain bricks are made into a cube with dimensions of length × width × height = $2 \times 2 \times 2$ cm. In order to ensure that the instantaneous signal of the explosion is transmitted to the strained brick without reflection, the wave impedance of the strained brick and the experimental model should be strictly consistent (Ma et al. 2001, Zong

2004). Therefore, the ratio of cement: sand: water is 1 : 1 : 0.5, three of them are involved, and the curing time is 28 day. In order to measure the explosion stress effectively, the strain bricks are arranged 5 cm from the bottom of the blast hole and about 1 cm from the wall of the blast hole. Two BX120-4AA strain gauges with the resistance of 120 Ω and sensitivity coefficient of $(2.08 \pm 1)\%$ were attached to each strain brick vertically in radial and tangential directions. When the strain gauge is pasted, the surface of the specimen is polished in the direction of 45° with respect to the axial direction of the strain brick, so as to ensure that the surface of the specimen is smooth and free of embedded gravel. Then the specimen is pasted with 502 Glue. When the glue is bonded, the strain gauge is pasted in the correct position quickly, and excess glue is extruded to ensure good contact between the strain gauge and the strain brick.The strain brick model is shown in Fig. 4.
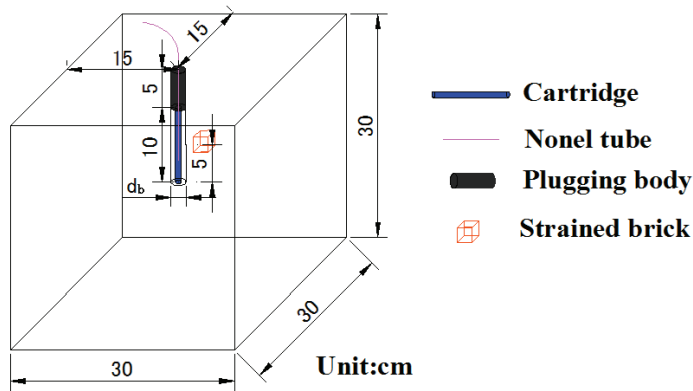

Fig. 2. Layout of model and measuring point
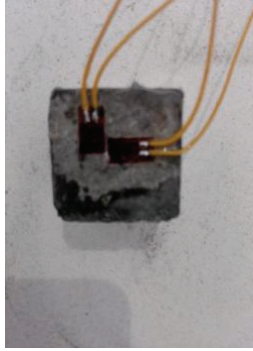

Fig. 3. Concrete model

Fig. 4. Strain brick model

According to the same proportion and manufacturing process, three specimens were made for the study of physical and mechanical properties. The specimens were cylindrical in appearance, with a bottom diameter of 5 cm and a height of 10 cm. After curing for 28 days, the relevant physical and mechanical properties were tested and the main mechanical parameters of the concrete model were obtained as shown in Table 1.

Table 1. Mechanical parameters of concrete mode

Test block number	Density [kg·m^{-3}]	Longitudinal wave velocity [m·s^{-1}]	Elastic modulus GPa	Compressive strength MPa	Poisson ratio
1	2247.12	3115	26.44	20.32	0.22
2	2153.24	3067	25.85	30.08	0.23
3	2177.00	3139	24.50	20.16	0.24
Average value	2192.45	3100	25.50	23.52	0.23

3.3. EXPERIMENTAL METHODS

Because of the small size of the model, the change of explosive charge has a great influence on the blasting effect, so it is difficult to design the gradient of explosive charge for effect comparison. Therefore, the control variables in this experiment make the charge diameter, charge amount, hole depth, hole blockage are the same in each group. The radial decoupling coefficient of air is changed by changing the hole diameter. As shown in Fig. 5, the diameter of the charge after special treatment is 0.8cm. When the hole diameter is 1.0, 1.2, 1.4, 1.6 and 1.8 cm, the corresponding decoupling coefficientsare 1.25, 1.50, 1.75, 2.00 and 2.25, respectively. Under the condition of five decoupling coefficients, air and water are used as decoupling medium, and other influencing factors remain the same. The strain data of the blasting process are col-

lected, and the peak pressure at the hole wall of the radial decoupling charge of the different medium is analyzed.

Fig. 5.The charge after special treatment

3.4. EXPERIMENTAL RESULTS

Each model is equipped with one detonator containing 1.0 g PETN, and the blast hole filling material is mixed with fine sand and 502 Glue. Test models filled with air medium and water medium and with decoupling coefficients of 1.25, 1.50, 1.75, 2.00 and 2.25 were blasted, respectively, and the data of explosion stress distribution of air and water radial decoupling charge were obtained, as shown in Table 2.

Table 2. Blasting experiments results of stress field for air and water radial decouple charge

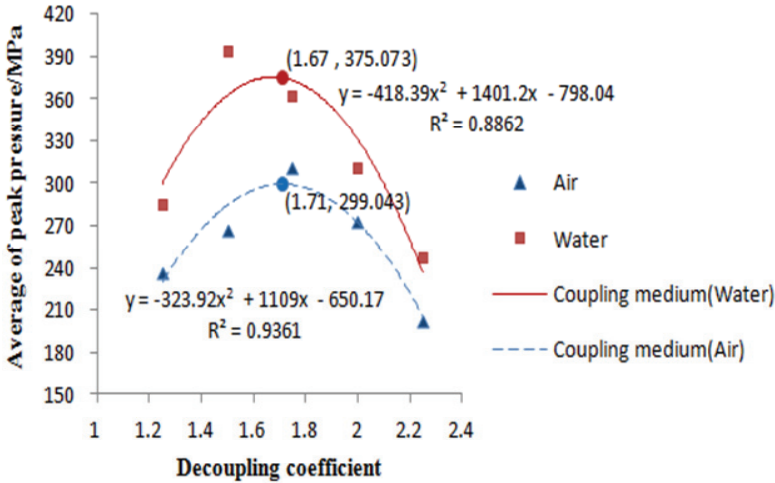| Decoupling coefficient, K_d	Coupling medium	Peak voltage, V		Peak strain, $\mu\varepsilon$		Average of peak strain, $\mu\varepsilon$	Average of peak pressure, MPa
		radial direction	tangential direction	radial direction	Tangential direction		
1.25	air	0.985	0.872	9850	8720	9285	236.768
	water	1.224	1.153	12240	11530	11185	285.218
1.50	air	1.115	0.979	11150	9790	10470	266.985
	water	1.624	1.471	16240	14710	15475	394.613
1.75	air	1.295	1.143	12950	11430	12190	310.845
	water	1.508	1.340	15080	13400	14240	363.120
2.00	air	1.141	1.005	11410	10050	10730	273.615
	water	1.366	1.074	13660	10740	12200	311.100
2.25	air	0.832	0.757	8320	7570	7945	202.598
	water	1.044	0.902	10440	9020	9730	248.115

Fig. 6. Coupling coefficient and average of peak pressure fitting effect map

After linear fitting of the actual data measured by AFT-0957-8 super-dynamic strain gauge, the fitting formula of radial air-decoupling charge is as follows:

$$y = -323.92x^2 + 1109x - 650.17 .$$ (12)

After linear fitting of the actual data measured by AFT-0957-8 super-dynamic strain gauge, the fitting formula of radial water-decoupling charge is as follows:

$$y = -418.39x^2 + 1401.2x - 798.04 ,$$ (13)

where: x is the decoupling coefficient, y is the mean peak pressure, MPa.

Combined with Table 2 and Fig. 6, it can be seen that when the decoupling coefficient Δ is the same, the mean peak pressure of radial water-decoupling charge blasting is larger than that of air-decoupling charge structure, which is consistent with the theoretical deduction results, indicating that under air-decoupling charge, the compressed air in the axial direction of the hole consumes a large amount of energy, resulting in low stress and strain. Under the condition of different medium decoupling charge, the peak pressure mean value and decoupling coefficient have a convex curve function relationship (as shown in Fig. 6), that is, there must be an optimal decoupling coefficient, and the peak pressure mean value reaches the maximum. The formula (12) and the Formula (13) are solved respectively, and the theoretical optimum air decoupling coefficient $\Delta = 1.71$ and the optimum water decoupling coefficient $\Delta = 1.67$ are obtained. The optimum air decoupling coefficient and the mean value of the peak pressure are compared with each other. When the same peak pressure is reached, the water decoupling coefficient is small, and the borehole hole diameter required by the blast hole is smaller than that of the air decoupling charge. At that same decouple coeffi-

cient, the peak pressure of water-decoupling charge is high, which indicates that the energy acting on the experimental model is great than that of air-decoupling charge.

4. TEST RESULTS AND ANALYSIS OF BLASTING LUMPINESS

4.1. RESULTS OF BLASTING LUMPINESS TEST

In this experiment, the single hole initiation method was used, and the fragmentation of each blast hole was measured by the mesh size method. As shown in Fig. 7, the screening tool is a seven-layer screening framework consisting of seven honeycomb panels with circular holes of different diameters, the diameter of which decreases from top to bottom. The selected fragments of different sizes were weighed by electronic scales, converted into volumes and compared with the funnel volume. Because the upper part of the hole is not covered in advance and some rock fragments are thrown out in the form of flying rocks, the experimental results are measured by the percentage of lumpiness and the volume of the blasting funnel. Specific lumpiness data is shown in Table 3.

Fig. 7. Screening tool

The results of blasting lumpiness obtained from concrete model blasting experiments are statistically analyzed by using the *G–G–S* distribution function.

The *G–G–S* distribution function is:

$$y = 100\left(\frac{x}{x_m}\right)^n,\qquad(14)$$

where: y is the cumulative percentage under screen, %, x is the size of the block, mm, n is the uniformity index of lumpiness distribution, x_m is the maximum lumpiness, mm.

Table 3. Different coupling media blasting experiment lumpiness degree percentage (y/%)

Coupling medium	Lumpiness degree, mm						
	<10	<15	<20	<25	<30	<35	<40
Air	7.26	11.62	14.97	19.17	30.86	37.96	45.07
Water	9.37	18.49	23.15	29.37	38.69	48.40	58.10
Air	5.35	11.17	17.11	23.89	30.51	36.21	41.91
Water	11.31	25.09	32.86	42.57	53.64	60.19	66.74
Air	5.29	9.15	9.93	14.60	20.26	25.04	29.81
Water	11.50	22.76	29.95	35.09	44.51	48.64	52.76
Air	3.07	6.23	8.22	11.91	16.40	19.60	22.80
Water	8.98	15.68	18.69	23.73	34.80	40.63	46.45
Air	3.28	4.79	6.37	10.06	13.62	15.85	18.08
Water	11.89	20.63	24.03	31.06	44.90	50.05	55.19

In order to find the unknown x_m and n in the above distribution function, the linear regression analysis is adopted. Firstly, the nonlinear regression is transformed into linear regression, and then the regression formula G–G–S is obtained.

$$Y = AX + B,$$

$$Y = \ln y; \quad X = \ln x; \quad A = n; \quad B = \ln 100 - n \ln x_m.$$

Among them, the results of regression analysis of lumpiness distribution in air and water medium are shown in Table 4.

The blasting effect is preliminarily evaluated by using lumpiness statistics K_{50}, K_{80} and after blasting. The function expression is as follows:

$$K_{50} = x_m \left(\frac{1}{2} \right)^{1/n}, \tag{15}$$

$$K_{80} = x_m \left(\frac{4}{5} \right)^{1/n}, \tag{16}$$

K_{50} is used to characterize the average lumpiness size, the size of the screen hole through which 50% of the blasting stack can pass, mm, K_{80} is used to characterize the distribution of large block, refers to the size of the screen hole through which 80% of the blasting stack can pass, mm.

The test results of this paper will be applied to smooth blasting of cutting slope. After blasting, the earth and rock will be backfilled in road subgrade engineering. Generally, the size of filling material is not more than 40 cm. In this paper, the similarity ratio of model test is 1 : 10, so the block larger than 40 mm is defined as a large block.

The statistics of boulder yield is obtained by comparing the lumpiness weight with the total lumpiness weight after screening the lumpiness size, i.e., in Table 3, 100% minus the screen cumulative amount (%) of the lumpiness size grade less than 40 mm is used in the cumulative amount under the screen of the air-water coupling medium blasting lumpiness size distribution, and the result is the boulder yield.

Among them, the blasting lumpiness effect analysis statistics of different medium decoupling coefficients are shown in Table 5.

Table 4. Results of regression analysis of block distribution
under air and water medium

Decoupling coefficient, K_d	Coupling medium	G-G-S distribution	Correlation coefficient
1.25	Air	$y = 100(x/75.19)^{1.34}$	0.977
	Water	$y = 100(x/63.43)^{1.26}$	0.991
1.50	Air	$y = 100(x/68.03)^{1.48}$	0.993
	Water	$y = 100(x/51.94)^{1.24}$	0.974
1.75	Air	$y = 100(x/111.05)^{1.24}$	0.976
	Water	$y = 100(x/66.35)^{1.07}$	0.971
2.00	Air	$y = 100(x/109.95)^{1.44}$	0.995
	Water	$y = 100(x/77.48)^{1.18}$	0.985
2.25	Air	$y = 100(x/144.03)^{1.31}$	0.983
	Water	$y = 100(x/66.37)^{1.12}$	0.984

Table 5. Analysis and statistics of the effect of blasting lumpiness
of uncoupling coefficient under different media

Decoupling coefficient, K_d	Coupling medium	Uniform index, n	Maximum lumpiness, x_m	Average lumpiness, K_{50}	K_{80}	boulder yield, %
1.25	air	1.34	75.19	44.82	63.66	54.93
	water	1.26	63.43	36.59	53.14	41.90
1.50	air	1.48	68.03	42.59	58.51	58.09
	water	1.24	51.94	29.70	43.39	33.26
1.75	air	1.24	111.05	63.50	92.76	70.19
	water	1.07	66.35	34.71	53.86	47.24
2.00	air	1.44	109.95	67.94	94.17	77.20
	water	1.18	77.48	43.06	64.13	53.55
2.25	air	1.31	144.03	84.85	121.47	81.92
	water	1.12	66.37	35.74	54.38	44.81

4.2. ANALYSIS OF FRAMENTATION EFFECT OF BLASTING
WITH DIFFERENT DECOUPLING COEFFICIENT OF MEDIUMS

According to the statistical results of blasting lumpiness screening, the broken lines of the relationship between the decoupling coefficient and K_{50}, K_{80} and the boulder yield indicator are shown in Fig. 8.

(a) Relationship between K_{50}
and decoupling coefficient

(b) Relationship between K_{50}
and decoupling coefficient

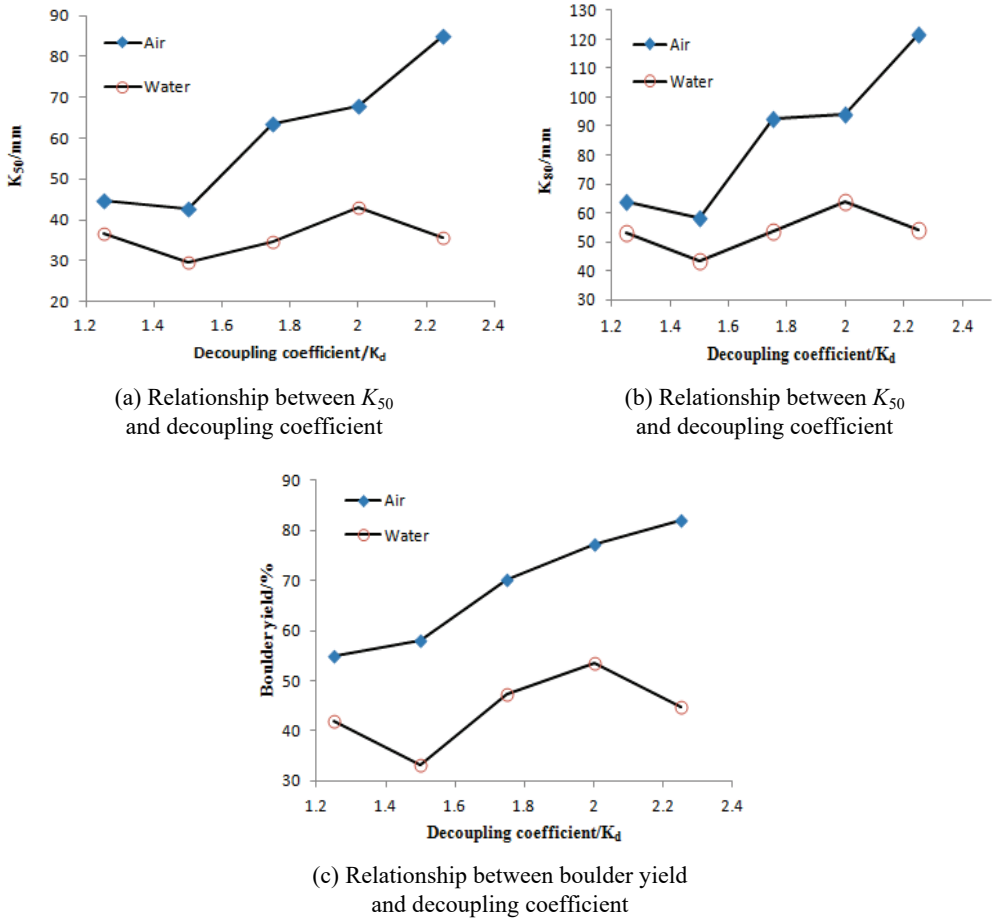(c) Relationship between boulder yield
and decoupling coefficient

Fig. 8. Relationship between lumpiness index and decoupling coefficient

As can be seen from Fig. 8, the evaluation index K_{50}, K_{80} and boulder yield of blasting lumpiness using water-decoupling charge is lower than that of air medium, which is consistent with the theoretical deduction result, that is, the initial impact pressure of hole wall of water-decoupling charge is higher than that of air-medium decoupling charge. In the same model test, the change trend of the lumpiness index of air medium

and water medium is the same, and the difference of the lumpiness index of air medium and water medium increases with the increase of the decoupling coefficient.

In Figure 8, the lumpiness index K_{50} and K_{80} of the overall fragmentation in the air medium tend to decrease at first and then increase. When $K_d = 1.50$, the minimum values of K_{50} and K_{80} are 42.59 mm and 58.51 mm, respectively, and the boulder yield in the air medium increases with the increase of the decoupling coefficient. With the increase of the decoupling coefficient, the lumpiness index K_{50}, K_{80} and boulder yield in the water medium decrease at first, then increase and then decrease. When $K_d = 1.50$, the minimum values of K_{50}, K_{80} and boulder yield in the water medium are 29.70 mm, 43.39 mm and 33.26%, respectively.

5. FIELD EXPERIMENT

Taking the smooth blasting construction of cutting as an example, the smooth blasting hole is drilled with a diameter of 115 mm, and the blasting is emulsified blasting. In order to improve the radial decoupling coefficient, a 70 mm diameter roll with a radial decoupling coefficient of 1.64 is used because the roll size is relatively fixed. The roll is fixed on the bamboo slice and placed into the hole, and the hole is filled with water and plugged. Connect the blasting network and initiate the blasting. The blasting effect is shown in Fig. 9.

As can be seen from Fig. 9, after blasting, the blasting lumpiness is small, the residual mark rate of the blasting hole is good, and there is no local crushing failure of the blasting hole.

Fig. 9. Smooth blasting effect of roller slope

6. CONCLUSIONS

This paper analyzes and compares the initial impact pressure of hole wall and the size of blasting lumpiness theoretically when air and water are used as coupling medium. Combined with blasting model test, strain data are collected by high-speed multi-channel dynamic stress testing system, and the lumpiness of model test is sieved and measured. The blasting lumpiness is analyzed by G-G-S distribution function. The conclusions are as follows:

1) From both theory and model test, it is concluded that the mean peak pressure of radial air-decoupling charge blasting is smaller than that of water-decoupling charge, which indicates that the axial compressed air consumes a lot of energy and causes low stress and strain under the condition of air-decoupling charge.

2) The size of blasting lumpiness of water-decoupling charge is smaller than that of air-decoupling charge both in theory and model test, which indicates that the utilization ratio of water-decoupling charge is higher than that of air medium, and the fragments are more uniform.

3) Combining the relation between the peak strain pressure and the decoupling coefficient, the optimal decoupling coefficients of air and water are 1.71 and 1.67, respectively, which indicates that the best blasting effect can be obtained by using the small hole diameter of the decoupling charge of water medium compared with the air-decoupling charge.

4) When $K_d = 1.50$, for the model of decoupling charge blasting in water medium, the three indexes of K_{50}, K_{80} and boulder yield are minimum; For the air-medium decoupling charge blasting model, the two evaluation indexes K_{50} and K_{80} are minimum, but in the actual blasting operation, the approximate optimal decoupling coefficient can be used in the blasting because of the limitation of the hole size and the diameter of the charge roll, which is not easy to change.

REFERENCES

ZONG Q., MENG E.J., 2003, *Influence of different kinds of hole charging structure on explosion energy transmission*, Chinese Journal of Rock Mechanics and Engineering, Vol. 22, No. 4, 643–644.

ZONG Q., LI Y.C., XU Y., 2004, *Preliminary discussion on shock pressure on hole wall when water-couple charge blasting in the hole*, Journal of Hydrodynanamics, Vol. 19, No. 5, 610–615.

ZONG Q., TIAN L., WANG H.B., 2012, *Study and application on rock damage range by blasting with water-decoupled charge*, Blasting, Vol. 29, No. 2, 42–46.

DAI J., QIAN Q.H., 2008, *Control of size of rock fragmentation by blasting*, Journal of Liaoning Technical University (Natural Science Edition), Vol. 27, No. 1, 54–56.

DU J.L., LUO Y.G., 2003, *Study of formation and propagation of shockwave with water-uncouple charge blasting in hole*, Rock and Soil Mechanics, No. (S2), 616–618.

DU J.L., LUO Q., ZONG Q., 2005, *Analysis on preliminary shock pressure on borehole of air-de-coupling charging*, Journal of Xi'an University of Science and Technology, Vol. 25, No. 3, 306–310.

WAN Y.L., WANG S.R., 2003, *Analyse of Impact Pressure About De-Coupling Charge*, Blasting, Vol. 18, No. 1, 13–15.

LING W.M., 2004, *Experimental Research on Explosion Pressure on the Wall of a Borehole in Rock*, Mining and Metallurgy, Vol. 13, No. 4, 13–16.

YAN G.B., YU Y.L., 2009, *Numerical simulation of air and water medium decoupling charge blasting*, Engineering Blasting, Vol. 15, No. 4, 13–19.

JIANG F.L., LI X.Y., LI G.H. et al., 2015, *Modification on calculation formula of rock mass blastability index based on rough set and nonlinear multiple regression*, Journal of Safety Science and Technology, Vol. 11, No. 1, 34–39.

LIU Y.Q., HE F.M., CHEN Y.Y., 2005, *Test and study on blasting crush rate and lump rate distribution*, Coal Engineering, Vol. 5, No. 4, 58–59.

CAI F., LIU Z.G., 2014, *Impact of water decoupling charging on the energy of stress waves generated by blast in the process of deep-hole presplit blast in coal-bed*, Journal of Safety Science and Technology, Vol. 10, No. 8, 16–21.

YANG X.L., ZHU Y., 1996, *Lumpiness problem in coal mining*, Coal, Vol. 5, No. 1, 33–35.

SUN L., REN Q.F., ZONG Q., 2010, *Application of water-decoupled charge in smooth blasting of coal mine rock tunnel*, Blasting, Vol. 27, No. 3, 25–28.

CHEN Z.B., CHEN Y.Y., 2015, *Distribution of rock fragment size in engineering blasting*, Safety in Coal Mines, Vol. 46, No. 9, 177–179.

HAN B., 2013, *Model experimental study and application of deep-hole blasting in hard rock for mine shaft*, Huainan, Anhui University of Science and Technology.

MA J.J., XIONG Z.Z., DUAN W.D. et al, 2001, *Theoretical testing study factors affecting parallel hole cut blasting*, Journal of University of Science and Technology (Natural Science Edition), Vol. 24, No. 2, 170–174.

ZONG Q., 2004, *Tunneling blasting parameters model experiment study on vertical well freezing soil*, Hefei, University of Science and Technology China.